Supporting Information

Tetrahedral DNA- directed core-satellite assembly as SERS sensor for mercury ions on single-nanoparticle level

Ning Feng[1], Jingjing Shen[1], Chang Li[1], Qianqian Zhao[1], Essy Kouadio Fodjo[2], Lei Zhang[1]*, Shufen Chen[1], Quli Fan[1], and Lianhui Wang[1]*

[1] State Key Laboratory of Organic Electronics and Information Displays, Institute of Advanced Materials (IAM), Nanjing University of Posts and Telecommunications, 9 Wenyuan Road, Nanjing 210023, China.

[2]Laboratory of constitution and reaction of matter, University of Felix Houphouet-Boigny, 22 BP 582 Abidjan 22, Cote d'Ivoire.

E-mail: iamlzhang@njupt.edu.cn; iamlhwang@njupt.edu.cn

1. Materials: gold (III) chloride trihydrate ($HAuCl_4$ $3H_2O$), ascorbic acid (AA), sodium borohydride ($NaBH_4$), cetyltrimethylammonium bromide (CTAB), 4-mercaptobenzoic acid (4-MBA), and cetyltrimethylammonium chloride (CTAC) were purchased from Sigma Aldrich. The mercury ions (Hg^{2+}) standard solution (0.01M) was prepared by dissolving 3.25g $Hg(NO_3)_2$ into 10 mL of 1M HNO_3 (Sinopharm Chemical Reagent, Shanghai, China). All oligonucleotides (tetra 1, tetra 2, tetra 3 and tetra 4) were purchased from Takara Biotechnology Co. Ltd. (Dalian, China) and the sequences were shown in Table S1. Milli-Q water (18.2 MΩ cm) was used in all experiments.

2. Instrumentation: Transmission electron microscope (TEM) images were acquired from a JEM-2010 instrument (Japan). Scanning electron microscope (SEM) images were performed by using an S-4800 instrument (Japan). Extinction spectra were obtained with a Shimadzu UV3600 spectrophotometer.

The dark-field microscopy (DFM) images, localized surface plasmon resonance (LSPR) and SERS scattering spectrum measurements were recorded by an inverted microscope (eclipse Ti-U, Nikon) equipped with a monochromator (Acton SP2358), a −75 °C cooled CCD detector (PIXIS 400BR: excelon, Princeton Instruments) and a 633 nm continuous-wave laser light (Spectra-Physics Excelsior, 100 mW). The microscope was equipped with a 60X objective lens, a dark-field condenser (0.8 < numerical aperture (NA) < 0.95), and a true-color digital camera (Nikon DS-fi2). The spectra were integrated through a 1 μm slit width.

3. Formation of tetrahedral DNA.

Tetrahedral DNA was synthesized based on the modified reported method.[1] In brief, four single strands (tetra 1, tetra 2, tetra 3 and tetra 4, the sequences shown in Table S1†) were dissolved in the TM buffer solution (20 mM Tris, 50 mM $MgCl_2$, pH 8.0) with equimolar quantities. The resulting mixture was heated to 95 °C for 5 min and then cooled to 4 °C for 5 min. For DNA assays: the tetrahedral DNA was analyzed using polyacrylamide gel electrophoresis (PAGE) in the TBE buffer solution (89 mM Tris, 89 mM boric acid, 2 mM EDTA, pH 8.3) at a constant current of 5 mA at 4 °C.

Table S1. The sequences of oligonucleotides (from 5'to 3'end) used in this work.

Oligonucleotide	Sequence (5-3)
Tetra 1	(CH2)6-S-S-(CH2)6-AGCATTACAGCTTGCTACACGATTCAGA
	CTTAGGAATGTTCGACATGCGAGGGTCCAATACCG
Tetra 2	(CH2)6-S-S-(CH2)6-ACGAACATTCCTAAGTCTGAAATTTATC
	ACCCGCCATAGTAGACGTATCACCAGGCAGTTGAG
Tetra 3	(CH2)6-S-S-(CH2)6-ACGTGTAGCAAGCTGTAATCGACGTTCTTTC
	TTCCCCTTGTTTGTTGTACTATGGCGGGTGATAAA

Tetra 4	ACGGTATTGGACCCTCGCATGACTCAACTGCCTGGTGATACGA(A)15

4. Characterization of the tetrahedral DNA.

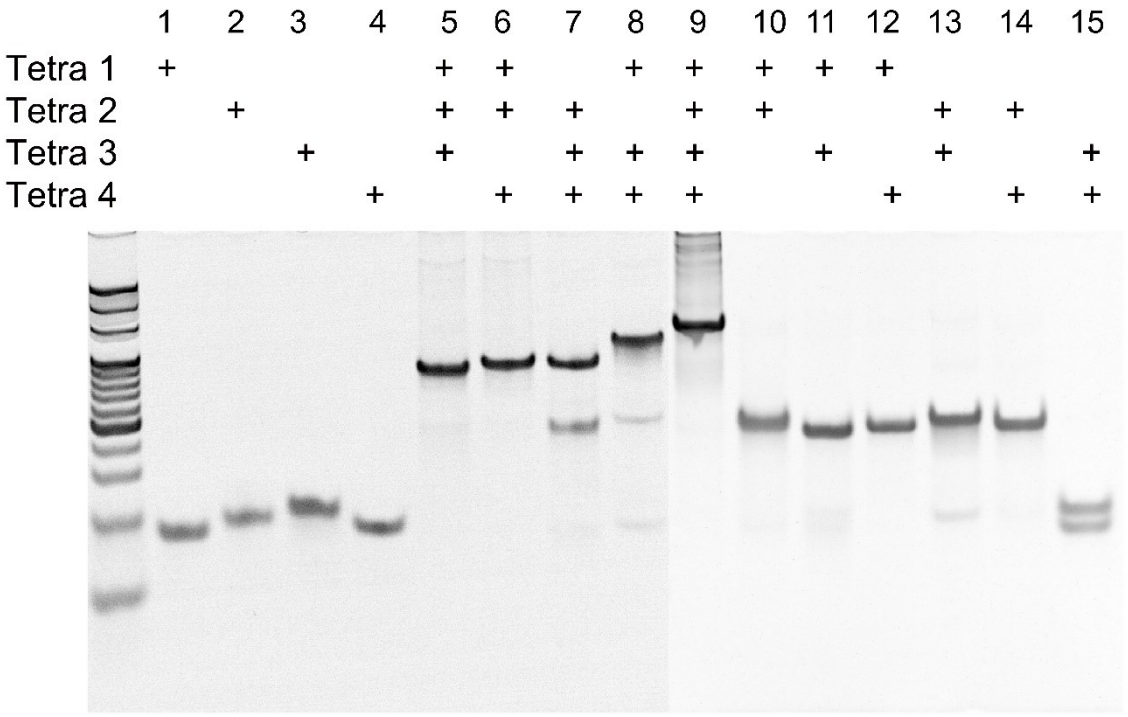

Fig. S1. Native gel electrophoretic analysis of tetrahedral DNA formation in TM buffer.

5. Synthesis of Surfactant-Stabilized satellite AuNPs.

Spherical CTAC-stabilized satellite gold nanoparticles (AuNPs) were synthesized by the seed-mediated growth method.[2] For the synthesis of 3 nm AuNPs, a HAuCl4 solution (0.01 M, 0.25 mL) was first mixed with a CTAB solution (0.1 M, 9.75 mL), followed by the rapid injection of a freshly-prepared, ice-cold $NaBH_4$ solution (0.01 M, 0.60 mL) under vigorous stirring. The resultant solution was kept under gentle stirring for 3 h at room temperature.

For the synthesis of CTAC-capped Au seeds, 150 μL of aqueous HAuCl4 solution (10 mM), 6 mL of aqueous CTAC solution (0.1 M) and 1.5 mL of aqueous AA solution (0.1 M) were mixed, followed by adding 30 μL of the 3 nm AuNPs. The final mixture turned from colorless into the red within 1 min, indicating the formation of CTAC-capped Au seeds.

108 μL of aqueous $HAuCl_4$ solution (10 mM), 8 mL of aqueous CTAC solution (0.1 M) and 1.5 mL of aqueous AA solution (0.1 M) were mixed, followed by adding 1 mL of CTAC-capped Au seeds. The final mixture turned from colorless into the red within 1 min, indicating the formation of satellite AuNPs.

6. Synthesis of Surfactant-Stabilized core AuNPs.

Core AuNPs were synthesized by using the seed-growth method following the previously reported method.[3] At first, 3 nm AuNPs were prepared by rapidly injecting the 0.6 mL freshly-prepared, ice-cold $NaBH_4$ solution (0.01 M) into the mixture solution composed of 0.25 mL $HAuCl_4$ solution (0.01 M) and 9.75 mL of CTAC solution (0.1 M), and then rapid stirring the resultant solution for 3 min. To ensure complete decomposition of the excess $NaBH_4$, the resultant solution was kept undisturbed for 3 h at room temperature.

For the synthesis of Au seeds, 487.5 μL of aqueous CTAB solution (0.01M) was firstly diluted with 9.5 mL of ultrapure water, followed by the addition of 750 μL of 0.1M AA and 200 μL of aqueous $HAuCl_4$ solution (0.01M). Afterward, 60 μL of 3 nm AuNPs solution was injected into the solution and then rapid stirring the seed solution for 3 min. Finally, the resultant solution was left undisturbed at room temperature for 12 h. The obtained Au seeds were centrifuged and redispersed in ultrapure water.

The Au nanopolyhedrons were grown by the seed-mediated method. Briefly, 110 μL Au seeds solution was first added into 3 mL of aqueous CTAC solution (0.025 M), followed by the addition of 150 μL of aqueous $HAuCl_4$ solution (0.01M) and 75 μL of 0.1M AA. The

mixture solution was kept in the air bath shaker (45 °C, 160 revolutions per minute) for 2 h. The obtained Au nanopolyhedrons were centrifuged and redispersed in a CTAB solution (0.02 M, 3 mL).

The core AuNPs were produced by oxidizing the obtained Au nanopolyhedrons with CTAB and $HAuCl_4$. Briefly, the Au nanopolyhedrons in CTAB solutions were mixed with a $HAuCl_4$ solution (0.01 M, 20 µL). The resultant mixture solution was kept in the air bath shaker (45 °C, 160 revolutions per minute) for 2 h. The obtained core AuNPs were centrifuged and then redispersed in ultrapure water.

7. Characterization of satellite AuNPs and core AuNPs.

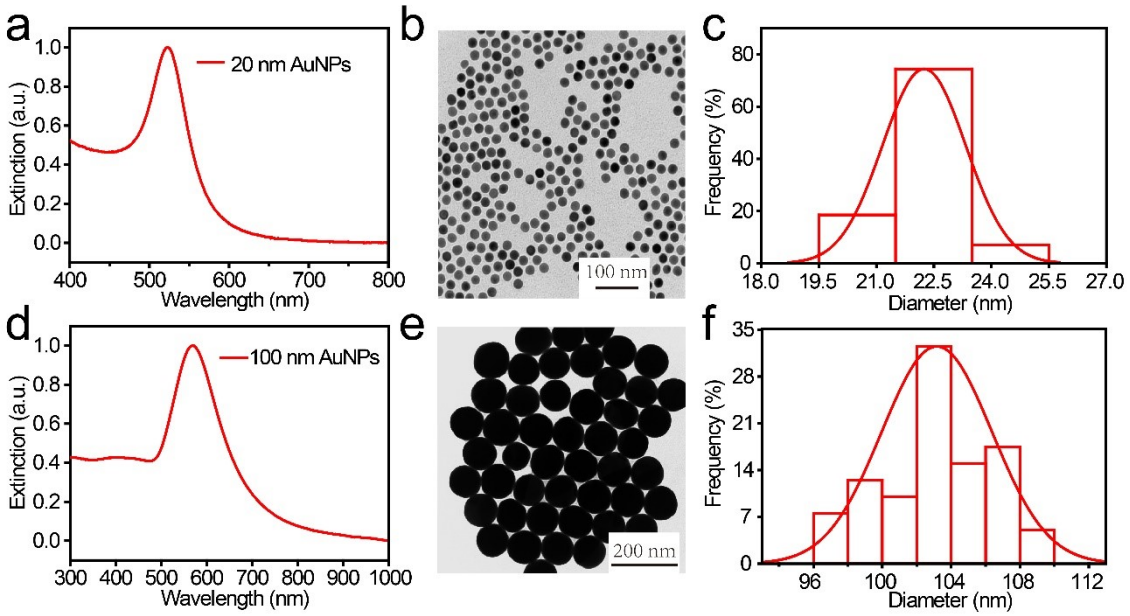

Fig. S2. Normalized extinction spectra of satellite AuNPs (a) and core AuNPs (d). Typical TEM images of satellite (b) and core (e) AuNPs. The diameter distribution of satellite (c) and core (f) AuNPs.

8. Characterization of SERS spectrum.

The SERS spectrum of individual nanoparticle was performed by using the DFM-correlated Raman spectroscopy setup (Fig. S3†). Briefly, the position of the individual particle was located by using the DFM image, following the light pathway was switched with a laser source instead of the white light, and then the corresponding SERS spectra were captured by using Raman spectroscopy. In this study, the SERS spectrum of individual core-satellite nanostructure was collected at an excitation wavelength of 633 nm, 29.2 µW of laser power and captured for 10 seconds. Figure S4a† depicts a typical SERS spectrum detected from individual core-satellite nanostructure. The characteristic Raman peak of 4-MBA at 1072 and 1583 cm^{-1}, which are assigned to v_{8a} and v_{12} aromatic ring vibrations, can be seen clearly.[4] In order to verify the SERS spectra of the individual particle, we characterized the morphology of individual nanoparticle via in-situ SEM after the optical measurement. Figure S4b† presents the DFM image of the corresponding individual core-satellite nanostructure immobilized on ITO glass. With the assistance of in-situ SEM image (Fig. S4c†), the precise position correlates the spectra of individual nanostructure with its DFM image by making rounded rectangle identifiable markings for readily recognizing the selected area. The in-situ SEM images of the selected area confirmed that the SERS spectrum was collected from the individual nanoparticle.

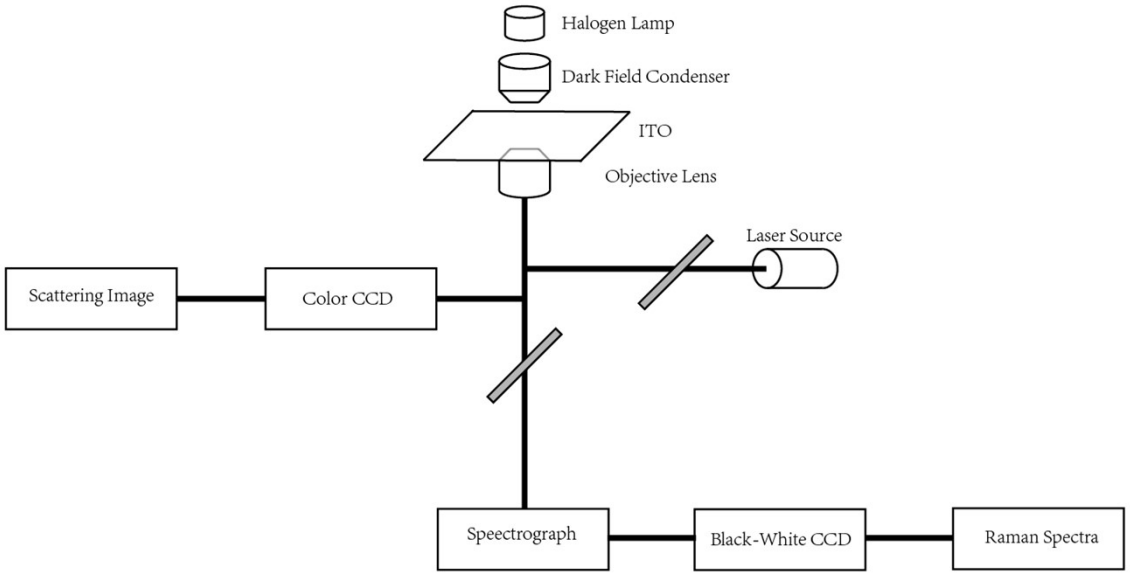

Fig. S3. Schematic diagram of DFM-correlated Raman spectroscopy for in situ single plasmonic nanostructure detection.

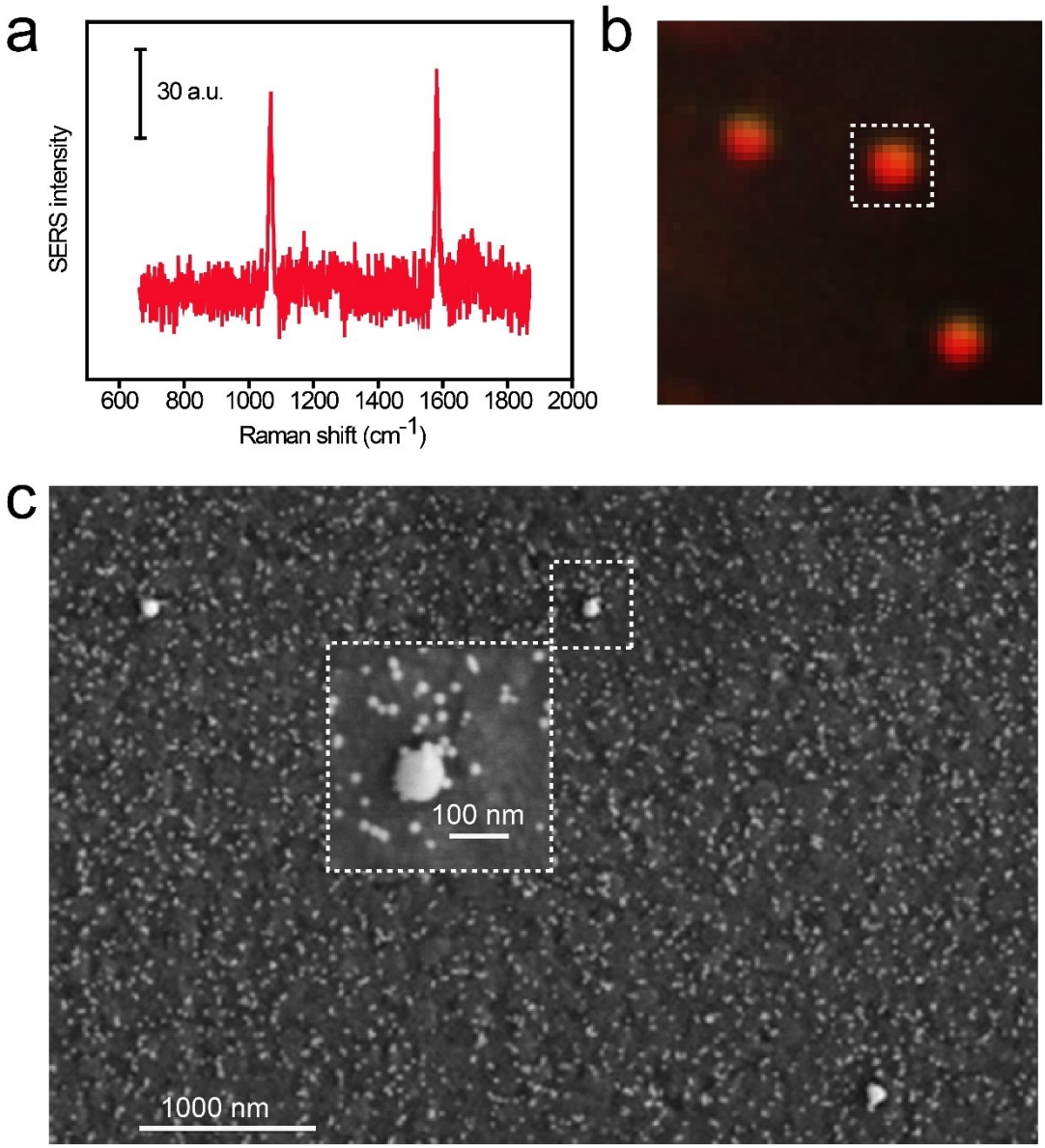

Fig. S4. (a) Representative SERS spectra of the individual core-satellite nanostructure. (b) DFM image of the core-satellite nanostructures on an ITO glass slide. (c) In situ SEM image of the selected area core-satellite nanostructure in DFM image. Insert: the enlarged SEM image of the selected area core-satellite nanostructure in DFM image.

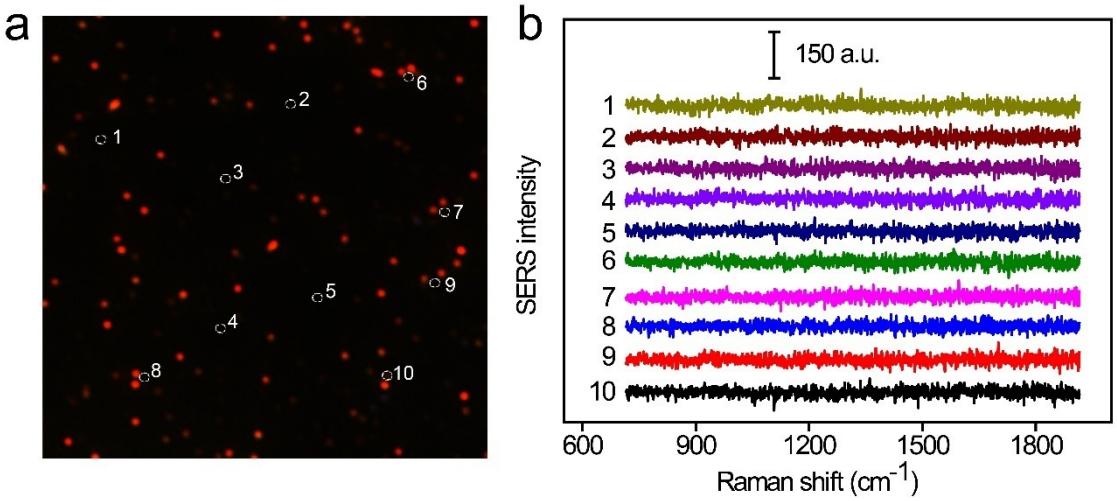

Fig. S5. (a) Representative DFM images of core-satellite nanostructure on ITO glass slide. The blank spot was marked by the white circle. (b) SERS spectra collected from 10 random blank spots on ITO glass slide. The labels of 1-10 in all of the panels correspond to the blank spots labeling of 1-10 shown in (a), respectively.

9. FDTD simulations.

FDTD treats Max Well equations as a finite differential equation in the scale of both time and space, and the software package FDTD Solution (version: 8.7.1072, Lumerical Solutions Inc, Vancouver Canada) was used to carry out the FDTD simulations. In the process of computational calculations, the incident light is circularly polarized with the wavelength ranging from 300 to 800 nm and the mesh sizes in x, y, z directions were all fixed to 0.1 nm. Perfectly matched layer (PML) absorbing boundary were used in all directions. To be consistent with the experiments, the surrounding environment (water) of the refractive index was set to be 1.33. All materials used the data from the model of Palik.[5]

Five structure models, as shown in Fig. S6†, with four satellite AuNP (20 nm in diameter) distributed around the core AuNP (100 nm in diameter) were constructed. As the satellite AuNP sequentially closing to the core AuNP, the gap distance changes from 4.5 to 1.2 nm. For simplicity, the contribution of DNA strands and glass slides was ignored.

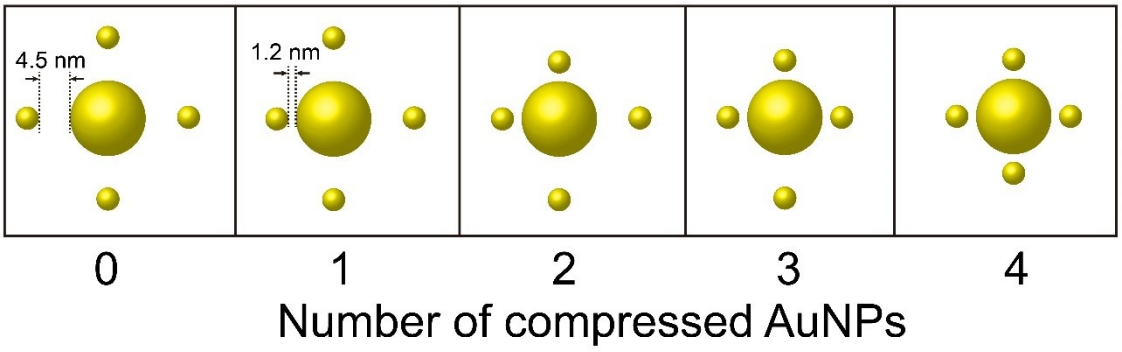

Fig. S6. Five models for the FDTD simulation. The labels of 0-4 correspond to the number of compressed satellite AuNPs.

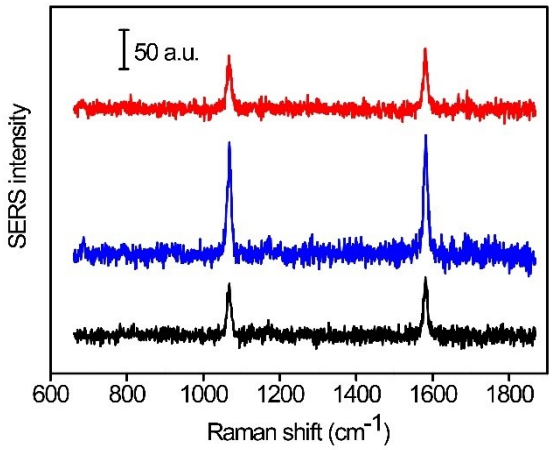

Fig. S7. SERS spectra of individual core-satellite assembly. The black curve represents the SERS spectra of the individual core-satellite assembly before the addition of 100 nM Hg^{2+}. The blue curve represents the SERS spectra of the individual core-satellite assembly after the addition of 100 nM Hg^{2+}. The red curve represents the SERS spectra of the individual core-satellite assembly after the addition of I^- ion (1 μM) at 10 minutes after treating with 100 nM Hg^{2+}.

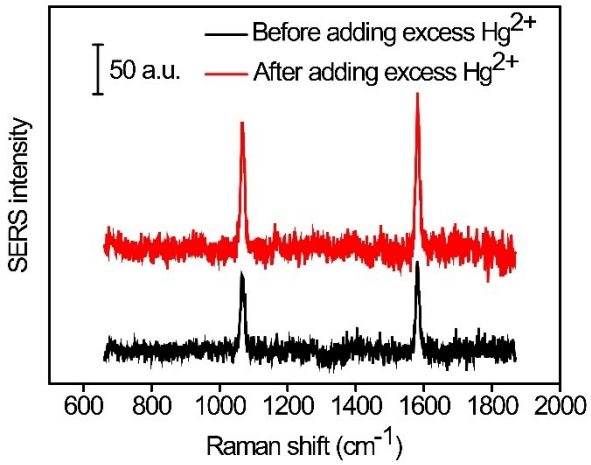

Fig. S8. Typical SERS spectra of 4-MBA attached to Au dimer before and after adding excess Hg^{2+}. 200 μL of Au dimer solution was pipetted onto the surface of the AuNP modified ITO glass slide. Then, excess Hg^{2+} was dropped into the Au dimer solution and incubated for 10 min. The SERS characterization was conducted in the liquid state before and after adding excess Hg^{2+}.

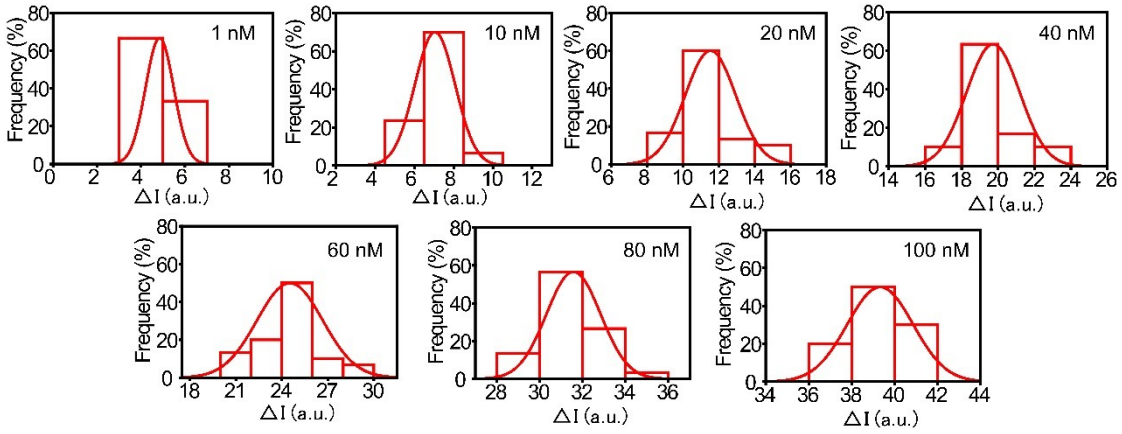

Fig. S9. Distributions of SERS intensity variation with the addition of various concentrations of Hg^{2+} (1, 10, 20, 40, 60, 80 and 100 nM).

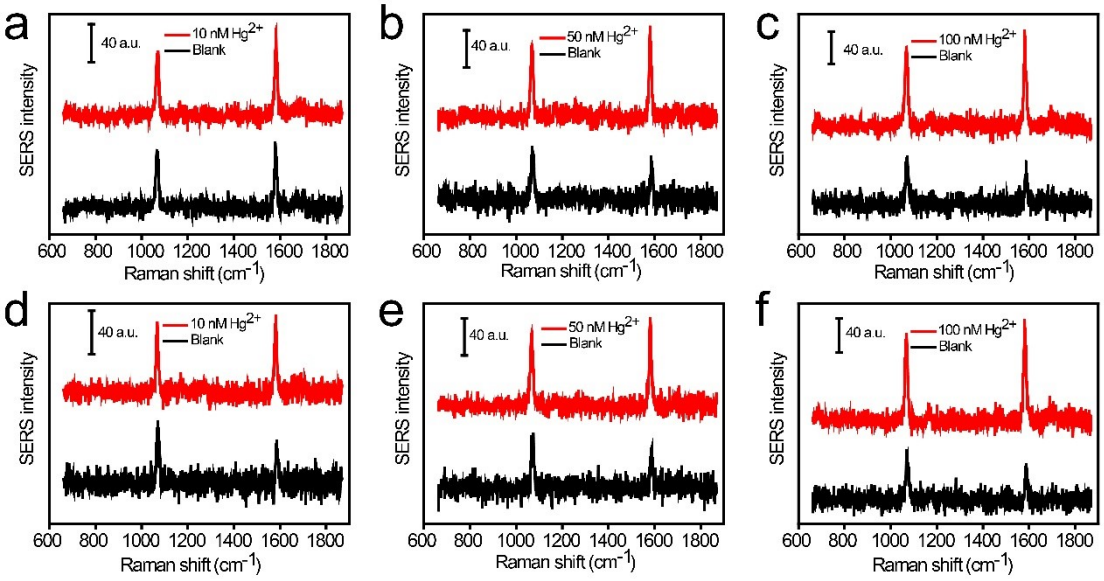

Fig. S10. SERS spectra of the core-satellite nanostructure exposed to 10 (a), 50 (b) and 100 nM Hg^{2+} (c) in tap water. SERS spectra of the core-satellite nanostructure exposed to 10 (d), 50 (e) and 100 nM Hg^{2+} (f) in lake water.

Table S2. Comparison of Assay Method for detecting Hg^{2+} ions.

Target Ions	Method	The detection limit	Ref
Hg^{2+}	electrochemistry	13.5 nM	Ref[6]
Hg^{2+}	fluorescence	9.2 nM	Ref[7]
Hg^{2+}	electrochemistry	1.8 nM	Ref[8]
Hg^{2+}	SERS	5 nM	Ref[9]
Hg^{2+}	SERS	7.9 nM	Ref[10]
Hg^{2+}	SERS	0.36 nM	Our results

REFERENCES

1. H. Pei, N. Lu, Y. Wen, S. Song, Y. Liu, H. Yan and C. Fan, *Adv. Mater.*, 2010, **22**, 4754-4758.
2. Y. Tian, Z. Shuai, J. Shen, L. Zhang, S. Chen, C. Song, B. Zhao, Q. Fan and L. Wang, *Small*, 2018, **14**, 1800669.
3. Q. Ruan, L. Shao, Y. Shu, J. Wang and H. Wu, *Adv. Opt. Mater.*, 2014, **2**, 65-73.
4. A. Michota and J. Bukowska, *J. Raman. Spectrosc.*, 2003, **34**, 21-25.
5. W. Choyke and E. D. Palik, *Palik (ed.), Academic Press, Inc*, 1985, **587**.
6. P. Veerakumar, G. Jaysiva, S.-M. Chen and K.-C. Lin, *ACS Appl. Mater. Inter*, 2022, **14**, 5908-5920.
7. Y. Zhang, S. Guo, Z. Jiang, G. Mao, X. Ji and Z. He, *Anal. Chem.*, 2018, **90**, 9796-9804.
8. X. Guo, J. Huang, Y. Wei, Q. Zeng and L. Wang, *J. Hazard. Mater.*, 2020, **381**, 120969.
9. X. Zhao, S. Campbell, P. Z. El-Khoury, Y. Jia, G. Q. Wallace, A. Claing, C. G. Bazuin and J.-F. Masson, *ACS Sens.*, 2021, **6**, 1649-1662.
10. D. S. Franciscato, T. A. Matias, J. Shinohara, J. M. Gonçalves, N. P. Coelho, C. S. Fernandes, E. A. Basso, H. S. Nakatani, K. Araki, H. E. Toma and V. R. de Souza, *Spectrochim. Acta. A*, 2018, **204**, 174-179.